



OPEN

A re-evaluation of the peak P – T conditions of eclogite-facies metamorphism of the Paleozoic Acatlán Complex (Mexico) reveals deeper subduction

D. Hernández-Uribe

Eclogites in the Acatlán Complex, southern Mexico, record the subduction history of the complex. Previous studies indicate that the proto-Acatlán Complex reached < 50 km depth during subduction. Yet, a recent study reported higher pressures for a single eclogite, questioning the maximum depth reached by the complex during subduction. In this work, I re-calculate eclogite pressure and temperature (P – T) conditions using thermobarometric methods applicable to eclogite-facies mafic rocks to a set of eclogites cropping out throughout the high-pressure belt of the Acatlán Complex—the Piaxtla Suite. I find that Acatlán eclogites record substantially—and systematically—greater pressures than previously reported. Calculations show that eclogites from the central part of the Piaxtla Suite (in the Piaxtla area) record consistent pressures of ~ 2.0 GPa and temperatures ranging between 460 and 675 °C. Eclogites from the northern part of the Piaxtla Suite (Mimilulco and Santa Cruz Organal areas) lack phengite, thus pressures were not calculated; temperatures calculated for these rocks at a fixed pressure (2.0 GPa) yield contrasting temperatures (511 °C and 870 °C, respectively). Mimilulco eclogite likely records similar pressures (~ 2.0 GPa) to other Piaxtla eclogites, whereas the pressures of Santa Cruz Organal eclogites might have been different, and likely experiencing a different thermal history compared to the rest of the eclogites from the Piaxtla Suite. Overall, these results indicate that the Acatlán Complex subducted to greater depths than previously thought implying a faster burial—exhumation cycle of the proto-Acatlán Complex.

Orogenic eclogites record key evidence of subduction-related processes and serve as important markers to identify paleo-subduction zones^{1–3}. This type of eclogites occurs in two different convergent-margin regimes, namely the Pacific- and collision-type orogens. Pacific-type eclogites form along colder geotherms compared to collision-type eclogites, reach slightly lower peak pressures (2.0–2.3 GPa) than collision-type eclogites (> 2.3 GPa), and exhume at different rates than collision-type eclogites^{3,4}. Therefore, constraining the pressure and temperature (P – T) evolution of eclogites is crucial for characterizing orogens, and specifically, for quantifying their burial—exhumation cycle.

The Acatlán Complex, southeastern Mexico (Fig. 1), exposes Paleozoic metamorphic rocks of various grades, including high-pressure (HP) lithologies such as chloritoid–rutile–phengite micaschists, garnet–rutile–phengite orthogneisses, garnet–epidote blueschists, and amphibole–phengite eclogites⁵. Eclogites in the Acatlán Complex represent the deepest subducted portions of the complex. A recent study⁶ reported maximum subduction depths of ~ 70 km—i.e. ~ 22–38 km higher than previously suggested for the Complex^{7–12}, questioning accepted geodynamic models and exhumation rates for the Acatlán Complex^{13,14}.

In this contribution, I re-evaluate the eclogite-facies metamorphism in the Acatlán Complex. For this, I calculated eclogite P – T conditions from different localities within the Acatlán Complex to evaluate whether the complex indeed experienced deeper subduction than previously thought or that this finding represents a single deep exposure within the Acatlán Complex. Finally, I discuss the implications of these results for the subduction and exhumation rates of the Acatlán Complex during the Paleozoic as well as for eclogite thermobarometry.

Department of Earth and Environmental Sciences, University of Illinois Chicago, Chicago, IL 60607, USA. email: dav.hernandez.uribe@gmail.com

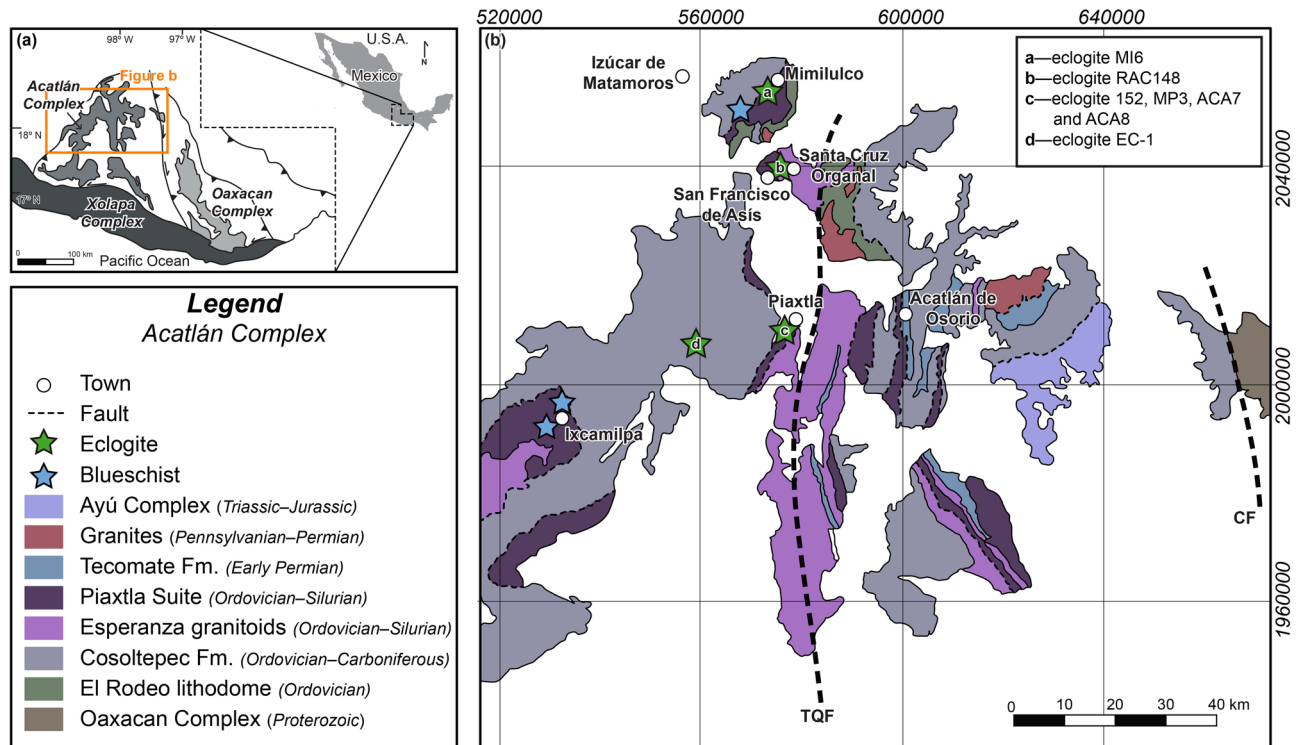


Figure 1. (a) Tectonostratigraphic terranes of southern Mexico. **(b)** Geological map of the Acatlán Complex. The green stars represent eclogite localities with the Piaxtla Suite (approximate locations). 152—Ortega-Gutiérrez⁷; MI6 and MP3—Meza-Figueroa et al.⁸; ACA7, ACA8, and RAC148—Vega-Granillo et al.¹⁰; EC-1—Hernández-Uribe et al.⁶; TQF—Tetla-Quicayán Fault; CF—Caltepec Fault. Modified from Hernández-Uribe et al.⁶.

Geological context

The Acatlán Complex, southern Mexico, is the largest exposure (~10,500 km²) of Paleozoic metamorphic rocks in Mexico, and one of the two localities in the country where eclogites and eclogite-facies rocks have been described so far^{5,15}.

The Acatlán Complex is a fault-bounded crystalline basement, bounded to the north by the Trans-Mexican Volcanic belt (Cenozoic), to the east by the Oaxacan Complex (Mesoproterozoic), to the south by the Xolapa Complex (Mesozoic), and to the west by the Guerrero-Morelos platform (Mesozoic)^{15–18} (Fig. 1). Since the work of Ortega-Gutiérrez¹⁵, the tectono-thermal evolution and stratigraphy of the polymetamorphic Acatlán Complex have been the subject of debate^{5,19–22}. Complications arise as the Acatlán Complex may record distinct orogenic cycles associated with opening and closure of the Iapetus, Rheic and Paleo-Pacific oceans^{20–23} leading to different subdivisions of the Complex, obscuring our understanding of its evolution.

This study focuses on the Piaxtla Suite (Fig. 1)—the HP belt of the Acatlán Complex where eclogite-facies metamorphism has been described. Details of the subdivision of the Acatlán Complex are described elsewhere^{5,19–22}. The Piaxtla Suite is a N–S trending HP belt comprised of metasediments, metabasites, metagranitoids, and serpentinized ultramafic bodies, which record variable metamorphic grade^{5,12,15,23,24} (Fig. 1). Different areas within the Piaxtla Suite record peak blueschist- to eclogite-facies conditions, and exhumation through the amphibolite and greenschist facies^{5–8,10,11,15}.

Acatlán eclogites

Eclogites *sensu lato* (the word eclogite here refers broadly to variably retrogressed mafic rocks with garnet, omphacitic clinopyroxene, and rutile) in the Piaxtla Suite crops out near the towns of Mimilulco, Las Minas, Santa Cruz Organal-San Francisco de Asís, and Piaxtla (Fig. 1). Eclogites display a peak mineral assemblage of Grt + Omp + Rt ± Ph ± Czo/Zo ± Qz ± Amp^{6–10,14}; this assemblage is replaced by amphibolite-(Amp + Pl + Ttn ± Czo/Zo) and greenschist-facies (Amp ± Chl) retrograde assemblages during exhumation^{6–10,14}. Existing *P–T* conditions calculated for eclogites (including variably retrogressed samples) vary depending on the area within the Piaxtla Suite. Previous works suggest *P–T* conditions of 1.1–1.5 GPa and 560 ± 60 °C in the area of Mimilulco⁸. In the Santa Cruz Organal area, eclogites record 1.5–1.7 GPa and 768–830 °C¹⁰, and in the Piaxtla area *P–T* conditions of 1.1–1.3 GPa and 491–609 °C^{7,8,10}. A new eclogite locality was reported by Hernández-Uribe et al.⁶ west of Piaxtla, and considered to record peak metamorphic conditions of ~2.2 GPa and ~690 °C. Other authors have reported “eclogite-facies” *P–T* conditions in amphibolites^{9,11}, that lack omphacitic clinopyroxene, garnet, and/or rutile, and in non-mafic lithologies such as rutile-bearing mica schists¹² and HP granitoids^{5,23}.

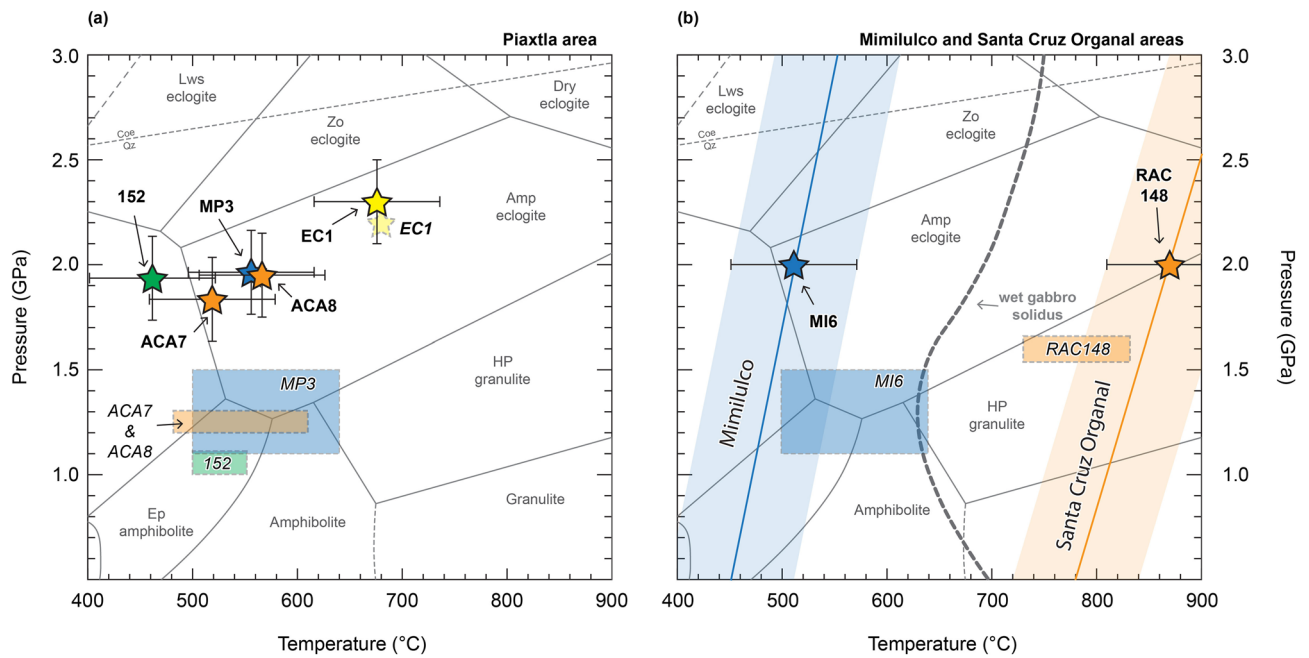


Figure 2. Pressure and temperature (P – T) conditions of Piactla Suite eclogites. (a) Piactla area and (b) Mimilulco and Santa Cruz Organal areas. The colored stars represent the mean P – T conditions and the error bars indicate the ± 0.2 GPa and ± 60 °C uncertainty associated to the thermobarometric methods (see Methods). The shaded colored rectangles with the sample number in italics correspond to the previously calculated P – T conditions for the same samples used in this study. The colors of the stars and boxes refer to: 152 (green)—Ortega-Gutiérrez⁷; MP3 and MI6 (blue)—Meza-Figueroa et al.⁸; ACA7, ACA8, and RAC148 (orange)—Vega-Granillo et al.¹⁰; EC-1 (yellow)—Hernández-Urbe et al.⁶.

Lu–Hf garnet–whole-rock geochronology from an amphibolitized eclogites in the Piactla area indicates that a single eclogite-facies metamorphism of the suite took place *c.* 351–353 Ma¹⁴, consistent with: (a) a Sm–Nd garnet–whole rock age of *c.* 388 \pm 44 Ma²⁵ (sample near town of Xayacatlán); (b) U–Pb zircon ages in retrogressed eclogites and amphibolites (interpreted as former eclogites) in the Piactla²⁶ and San Francisco de Asís areas⁹; and (c) with amphibole ⁴⁰Ar/³⁹Ar ages of *c.* 342–344 from an amphibolite (“retrogressed eclogite” from the area of Piactla)¹³ and of *c.* 336 \pm 6 Ma of an eclogite from the Piactla area¹⁰. Other studies, however, suggest that the Acatlán Complex records more than one eclogite facies event^{10,19,22}. An amphibole ⁴⁰Ar/³⁹Ar age of *c.* 430 \pm 5 Ma reported from a retrogressed eclogite in the Santa Cruz Organal area was interpreted to date eclogite-facies metamorphism, followed by a *c.* 374 Ma ⁴⁰Ar/³⁹Ar phengite age in the same sample, interpreted to date cooling during exhumation¹⁰; however, the interpretation of the ⁴⁰Ar/³⁹Ar ages is disputed, as the samples display complex Ar spectra suggesting Ar excess or inheritance¹⁴.

Thermobarometry of Acatlán eclogites

To re-explore the eclogite-facies P – T conditions of the Piactla Suite in the Acatlán Complex, I applied thermobarometric methods suitable for eclogite-facies mafic rocks. There are four published studies (to my knowledge) with available compositions of garnet, omphacitic clinopyroxene, and phengite in the Piactla Suite, which result in three eclogite localities in the Acatlán Complex (Fig. 1). These include the Piactla area with samples 152⁷, MP3⁸, ACA7¹⁰, ACA8¹⁰, and EC-1⁶. Towards the north, localities include Mimilulco, with sample MI6⁸ and Santa Cruz Organal, with eclogite RAC148¹⁰. The study of Middleton et al.⁹, from the San Francisco de Asís area (near Santa Cruz Organal; Fig. 1), was not included here because the published clinopyroxene (inclusion in amphibole) composition is a non-omphacitic clinopyroxene.

Pressures were calculated using the garnet–clinopyroxene–phengite barometer of Ravna and Terry²⁷. Temperatures were obtained using the garnet–clinopyroxene thermometer calibrations of Ravna²⁸, Nakamura²⁹, and Sudholz et al.³⁰. While some of these thermobarometers have been available for several decades, their application for the Acatlán eclogites is still novel. For internal consistency, the reported results in the text and in Fig. 2 correspond to the calculated mean of the intersections between the Ravna and Terry²⁷ barometer and Ravna²⁸ thermometer (Table 1). Temperatures obtained from the Nakamura²⁹ and Sudholz et al.³⁰ calibrations are also given in Table 1. Details of the methodology and related uncertainties are provided in the Methods section.

Different eclogites from the Piactla area yield similar P – T conditions (Fig. 2a). Eclogite MP3 yields P – T conditions of 1.97 GPa and 555 °C, eclogites ACA7 and ACA8 yields conditions of 1.83 GPa and 519 °C and 1.94 GPa and 565 °C, respectively. Eclogite 152 yields P – T conditions of 1.94 GPa and 468 °C (Fig. 2a). Eclogite EC-1, from the new locality west to the area of Piactla, yields 2.3 GPa and 675 °C (Fig. 2a), the greatest of all the Acatlán Complex.

	P (GPa) ^a					T (°C) ^b					T (°C) ^c				T (°C) ^d			
	n	Max	Min	Mean	2σ	n	Max	Min	Mean	2σ	Max	Min	Mean	2σ	Max	Min	Mean	2σ
Piaxtla area																		
152	4	2.07	1.82	1.94	0.199	4	509	430	468	65	483	446	457	35	509	435	471	60
MP3	8	2.04	1.9	1.97	0.092	8	571	539	555	24	528	510	520	14	576	549	562	23
ACA7	8	1.88	1.79	1.83	0.077	8	525	512	519	11	547	529	536	18	600	571	586	28
ACA8	8	2.01	1.87	1.94	0.093	8	574	556	565	13	584	566	576	18	626	611	619	12
EC1	4	2.33	2.28	2.30	0.004	4	680	670	675	12	646	640	643	7	691	684	688	7
Mimilulcoand Santa Cruz Organal areas																		
MI6*	–	–	–	–	–	1	–	–	511	–	–	–	498	–	–	–	529	–
RAC148*	–	–	–	–	–	4	890	850	870	35	832	805	818	23	907	882	895	35

Table 1. Calculated $P - T$ conditions of Acatlán eclogites. *Temperatures calculated at 2.0 GPa. ^aRavna and Terry²⁷; ^bRavna²⁸; ^cNakamura²⁹; ^dSudholz et al.³⁰.

In contrast to the Piaxtla eclogites, the Mimilulco and Santa Cruz Organal eclogites yield contrasting temperature estimates (Fig. 2b); unfortunately, there are no phengite analyses from either localities, thus no new pressure estimates were calculated. The Mimilulco eclogite MI6 yields a garnet–clinopyroxene temperature of 511 °C at 2.0 GPa (only one garnet–clinopyroxene pair available⁸). By contrast, the Santa Cruz Organal eclogite RAC148 yields a temperature of 870 °C at 2.0 GPa (Fig. 2b).

Discussion

Comparison with previous studies. Temperatures calculated in this work are similar to previously published estimates for eclogites in different parts of the Acatlán Complex^{6–8,10} (Fig. 2). However, our barometric calculations show substantially—and systematically—higher pressures than previously calculated across the Acatlán Complex (Fig. 2). For instance, in the Piaxtla area, the calculated pressure is ~2.0 GPa for four different samples (eclogite 152, MP3, ACA7, and ACA8; Fig. 2) whereas previous studies^{7,8,10} suggested that the eclogite-facies metamorphic event in this area occurred at ~1.1–1.5 GPa; such estimates are different even when considering the ±0.2 GPa uncertainty related to the barometer (see Methods).

Unfortunately, the lack of phengite in the eclogites from the Mimilulco and Santa Cruz Organal areas precluded the recalculation of new pressures with the approach used in this work. Yet, there is no reason for why the 1.1–1.5 GPa for the Mimilulco eclogite and 1.5–1.7 GPa for the Santa Cruz Organal eclogite could not be higher than previously reported. For example, Meza-Figueroa et al.⁸ suggest that the Mimilulco eclogite (MI6) was metamorphosed at the same $P - T$ conditions than eclogite MP3 from Piaxtla⁸; thus the Mimilulco eclogite could also record pressures of ~2.0 GPa. By contrast, it is more challenging to infer a pressure for the Santa Cruz Organal eclogite, as $P - T$ conditions are not available for other eclogites near the area. Previous work in the San Francisco de Asís area (relatively near Santa Cruz Organal; Fig. 1) estimated pressures > 1.6 GPa⁹, similar to that calculated by Vega-Granillo et al.¹⁰ for the Santa Cruz Organal eclogite (1.5–1.7 GPa), but with contrasting temperatures (650–750 °C⁹ vs 768–830 °C¹⁰). The temperature mismatch between these studies may be explained either by the fact that eclogites in both localities experienced different $P - T$ conditions or due to the use of non-omphacitic clinopyroxene for the thermobarometry⁹. The fact that the Santa Cruz Organal eclogite records the highest temperature in the Acatlán Complex (Fig. 2 and Table 1) may suggest that the pressure could be different to other eclogites in the Piaxtla Suite as well.

A recent petrologic study combining phase-equilibrium modeling and Zr-in-rutile thermometry for an eclogite from a new locality west of Piaxtla area obtained conditions of ~2.2 GPa and ~690 °C⁶. Our thermobarometric calculations for the same eclogite sample (EC-1) yield similar $P - T$ conditions than previously calculated (Fig. 2; Table 1). Importantly, the agreement between the previous $P - T$ calculations from Hernández-Urbe et al.⁶ with the conditions obtained here, further support our findings for the other eclogites in different parts of the Acatlán Complex.

Implications for the geodynamic evolution. The difference between the previously reported pressures for all the complex and the contrastingly higher pressure in the new eclogite locality was interpreted to be an artifact due to differences in thermobarometric methods⁶. However, here, I obtained similar pressures from different parts of the Piaxtla Suite of the Acatlán Complex using conventional thermobarometric approaches (Fig. 2). Therefore, I argue that these new results indicate systematic deeper subduction than previously thought. If no errors are considered, the calculated pressures of ~1.9–2.3 GPa, and corresponding inferred depths (63–75 km; see methods for pressure-to-depth conversion) suggest that different areas within the complex record slightly different depths. On the other hand, if the uncertainties in the calculations are considered (±0.2 GPa, ±6–7 km), then the calculated pressures and inferred depths in this work converge suggesting the complex reached a similar depth during subduction.

Temperatures from the Piaxtla and Mimilulco areas are the same considering the ±60–100 °C uncertainty related to the thermometric calculations. However, the temperature calculated here and in a previous work¹⁰ for the Santa Cruz Organal eclogite indicate that this area records the highest temperature of any rocks in the Acatlán Complex (Fig. 2). The differences in calculated temperatures could suggest different locations of the proto-Acatlán

Complex within the subducting slab (i.e., hotter towards the slab top vs colder towards the bottom). Regardless of the temperature interpretation, the greatest depths obtained here situates the subducting proto-Acatlán Complex deeper than previously hypothesized by all the tectonic models for the region.

The greater pressures–depths calculated here for the eclogites imply a faster subduction–exhumation cycle for the Acatlán Complex. Simple tectonic-rate calculations for the Acatlán Complex were obtained by using: (a) the youngest depositional ages of the sediments above the mafic oceanic crust; (b) the greatest depth reached during subduction and related eclogite-facies age (considering a single event); as well as (c) the depth and time of exhumation. For calculating the burial rate, I use the youngest detrital zircon in a metapsammite in the Piaxtla Suite with an age of *c.* 365 Ma interpreted to represent the youngest depositional limit¹³. Coupled with the depth from this work (i.e. 75 km) and an eclogite-facies age of *c.* 353 Ma (Lu–Hf garnet–whole-rock¹³), I obtained a linear burial rate of ~6.3 mm/yr, well within the estimates of convergence rates of tectonic plates in subduction zones³¹. Furthermore, the eclogite-facies data obtained here combined with muscovite ⁴⁰Ar/³⁹Ar cooling age of *c.* 334 Ma in a retrogressed eclogite¹³ with amphibolite-facies *P–T* conditions of ~0.6 GPa⁸ equates to an exhumation rate of ~2.8 mm/yr, similar to other HP terranes worldwide³². In summary, these simple calculations indicate it took the proto-Acatlán Complex ~12 Myr to subduct to ~75 km depth, and ~19 Myr to return to crustal depths, resulting in a subduction–exhumation cycle of ~31 Myr. These calculations contrast and thus challenge models for the Acatlán Complex with slower subduction and exhumation rates. For example, a previous burial rate of 2.7 mm/yr¹³ and an exhumation rate of 2.4 mm/yr¹³ are 3.6 mm/yr and 0.8 mm/yr slower, respectively, than the ones calculated here. The discrepancy between the calculated burial–exhumation cycle may be explained by the input data, as the burial and exhumation rates are strongly dependent in the timing of both the formation of the eclogite protolith and the exhumation to crustal depths. However, regardless of these data, the thermobarometric and new depth calculations obtained in this work would unequivocally result in faster tectonic rates.

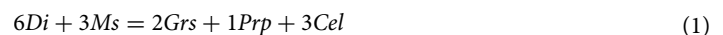
Implications for eclogite thermobarometry. The results presented here indicate that for the Acatlán eclogites, conventional thermobarometric methods, phase-equilibrium modeling⁶, and Zr-in-rutile thermometry⁶ yield consistent *P–T* conditions (Fig. 2a). While the uncertainties related to conventional thermobarometric methods (see Methods section) are considerably larger than the ones from other methods³³, I argue that in relatively well-equilibrated rocks, *P–T* estimates should be similar. Thus, as shown by other studies^{2,34,35}, the obtention of reliable *P–T* data needs to involve the application of different thermobarometric methods.

The temperatures obtained using different calibrations are the same including uncertainties (Table 1). The calibration from Sudhloz et al.³⁰ yields the highest temperatures compared to the other calibrations, whereas the Nakamura²⁹ calibration tend to yield the lowest temperature of all the thermometers (Table 1). Importantly, the Sudhloz et al.³⁰ calibration was parametrized from high-temperature experiments of mantle lithologies, potentially explaining why such temperatures are the highest. Yet, the mineral compositions from Acatlán eclogites are within the ranges recommended for that calibration (Supplementary Tables S1–S3). Further, from all the calibrations used here, only the Sudhloz et al.³⁰ thermometer includes a correction for the jadeite content in clinopyroxene, which is key for yielding reliable temperatures for subduction-related eclogites^{36,37}.

The comparison between the calculated temperatures in this work and the study of Hernández-Uribe et al.⁶ (which used Zr-in-rutile thermometry) indicates that the Sudhloz et al.³⁰ thermometer yields almost identical temperatures than the Zr-in-rutile thermometer (695 °C⁶ vs 688 °C). By contrast, such Zr-in-rutile temperatures differ the most from the Nakamura²⁹ temperature (695 °C⁶ vs 643 °C). Therefore, the comparison between independent approaches seems to suggest that the Sudhloz et al.³⁰ calibration may yield more reliable temperatures for subduction-related eclogites than the other Fe–Mg garnet–clinopyroxene thermometers.

Methods

Barometric calculations were done using the garnet–clinopyroxene–phengite barometer with the calibration of Ravna and Terry²⁷. The garnet–clinopyroxene–phengite barometer relies in the net transfer reaction between garnet, clinopyroxene, and phengite (mineral abbreviations follow Warr³⁸):



where the equilibrium constant (K_1) of this reaction can be expressed as:

$$K_1 = \frac{(a_{Prp}^{Grt})(a_{Grs}^{Grt})^2(a_{Cel}^{Ph})^3}{(a_{Di}^{Cpx})^6(a_{Ms}^{Ph})^3} \quad (2)$$

Temperatures were calculated using the garnet–clinopyroxene thermometer using the Ravna²⁸, Nakamura²⁹, and Sudholz et al.³⁰ calibrations. The garnet–clinopyroxene thermometer relies on the exchange of Fe²⁺ and Mg between garnet and clinopyroxene. The equilibrium Fe²⁺–Mg distribution coefficient (K_D) can be expressed as:

$$K_D = \frac{\left(\frac{Fe^{2+}}{Mg}\right)^{Grt}}{\left(\frac{Fe^{2+}}{Mg}\right)^{Cpx}} \quad (3)$$

Uncertainties related to the conventional thermobarometers applied here are commonly quoted to be ±0.2 GPa for the barometer^{27,39,40} and ±60 °C for the thermometer^{27,28,37}. For the latter, temperatures can be up ±100 °C due to the Fe³⁺ estimation in clinopyroxene⁴¹. In this work, Fe³⁺ in clinopyroxene calculated with the following

relation: $\text{Fe}^{3+} = \text{Na} - \text{Al} - \text{Cr}$. This Fe^{3+} recalculation scheme was used instead of the stoichiometric Fe^{3+} as the latter resulted in unrealistic lower garnet–clinopyroxene temperatures ($< 350^\circ\text{C}$).

For the P – T calculations, published garnet, clinopyroxene, and phengite chemical compositions^{6–8,10} were used from eclogites distributed along different portions of the Piaxtla Suite within the Acatlán Complex (Fig. 1; Supplementary Tables S1–S3). When provided, available petrological context in the publications (e.g., rims vs core and/or interpretations of peak vs retrograde), were considered for the P – T calculations. For samples MP3⁸, MI6⁸, and EC-1⁶, all the mineralogical data come from such papers. Data for eclogite 152⁷ was partially published by Ortega-Gutiérrez⁷; the complete analyses were kindly provided by the author. Similarly, data for ACA7, ACA8, and RAC148 was partially published by Vega-Granillo et al.¹⁰. Complete analyses were obtained from that author's doctoral dissertation. In this case, we only picked a pair of each mineral for the P – T calculations. All mineralogical analyses used for the thermobarometric calculations are given in Tables S1–S3 in the Supplementary Material.

Pressure-to-depth conversion uses a layered model assuming a total crustal thickness of 30 km, where the upper crust is 20 km and has a density of 2.8 g/cm³, and where the lower crust is 10 km and has a density of 2.9 g/cm³. The crust is followed by an upper mantle with density of 3.3 g/cm³. A greater crustal thickness results in greater subduction depths, whereas changes in the considered densities would have minor effects on the overall calculated depth. Tectonic overpressure was not considered in our pressure-to-depth calculations but deviation from lithostatic pressure is likely within the order of the depth uncertainty related to the barometric method used here⁴².

Data availability

All data used for the thermobarometric calculations are provided in Supplementary Information. The excel spreadsheet used the calculations is available at <https://doi.org/10.1111/j.1525-1314.2004.00534.x>.

Received: 26 October 2022; Accepted: 7 December 2022

Published online: 10 December 2022

References

1. Carswell, D. A. Eclogites and eclogite facies: Definitions and classifications. In *Eclogite Facies Rocks* (ed. Carswell, D. A.) 1–13 (Blackie and Son, 1990).
2. Hernández-Urbe, D., Mattinson, C. G. & Zhang, J. X. Phase equilibrium modelling and implications for P – T determinations of medium-temperature UHP eclogites, North Qaidam terrane, China. *J. Metamorph. Geol.* **36**, 1237–1261 (2018).
3. Tsujimori, T. & Mattinson, C. G. Eclogites in different tectonic settings. In *Encyclopedia of Geology* (eds Elias, S. & Alderton, D.) 561–568 (Academic Press, 2021).
4. Agard, P., Yamato, P., Jolivet, L. & Burov, E. Exhumation of oceanic blueschists and eclogites in subduction zones: Timing and mechanisms. *Earth. Sci. Rev.* **92**, 53–79 (2009).
5. Ortega-Gutiérrez, F. et al. The pre-Mesozoic metamorphic basement of Mexico, 1.5 billion years of crustal evolution. *Earth. Sci. Rev.* **183**, 2–37 (2018).
6. Hernández-Urbe, D., Gutiérrez-Aguilar, F., Mattinson, C. G., Palin, R. M. & Neill, O. K. A new record of deeper and colder subduction in the Acatlán complex, Mexico: Evidence from phase equilibrium modelling and Zr-in-rutile thermometry. *Lithos* **324**, 551–568 (2019).
7. Ortega-Gutiérrez, F. Nota preliminar sobre las eclogitas de Acatlán, Puebla. *Bol. Geol. Soc. Mex.* **35**, 1–6 (1974).
8. Meza-Figueroa, D., Ruiz, J., Talavera-Mendoza, O. & Ortega-Gutiérrez, F. Tectonometamorphic evolution of the Acatlan Complex eclogites (southern Mexico). *Can. J. Earth. Sci.* **40**, 27–44 (2003).
9. Middleton, M. et al. P – T – t constraints on exhumation following subduction in the Rheic Ocean from eclogitic rocks in the Acatlán Complex of southern Mexico. *Geol. S. Am. S.* **423**, 489–509 (2007).
10. Vega-Granillo, R. et al. Pressure-temperature-time evolution of Paleozoic high-pressure rocks of the Acatlán Complex (southern Mexico): Implications for the evolution of the Iapetus and Rheic Oceans. *Geol. Soc. Am. Bull.* **119**, 1249–1264 (2007).
11. Ramos-Arias, M. A., Keppie, J. D., Lee, J. K. W. & Ortega-Rivera, A. A Carboniferous high pressure/grade klippe in the western Acatlán Complex (southern Mexico): Implications for tectonothermal development and Pangean paleogeography. *Int. Geol. Rev.* **54**, 779–798 (2012).
12. Galaz, E. G., Keppie, J. D., Lee, J. K. W. & Ortega-Rivera, A. A high-pressure folded klippe at Tehuiztzingo on the western margin of an extrusion zone, Acatlán Complex, southern México. *Gondwana Res.* **23**, 641–660 (2013).
13. Keppie, J. D., Nance, R. D., Dostal, J., Lee, J. K. W. & Ortega-Rivera, A. Constraints on the subduction erosion/extrusion cycle in the Paleozoic Acatlán Complex of southern Mexico: Geochemistry and geochronology of the type Piaxtla Suite. *Gondwana Res.* **21**, 1050–1065 (2012).
14. Estrada-Carmona, J. et al. Lu–Hf geochronology of Mississippian high-pressure metamorphism in the Acatlán Complex, southern México. *Gondwana Res.* **34**, 174–186 (2016).
15. Ortega-Gutiérrez, F. Estratigrafía del Complejo Acatlán en la Mixteca Baja, estados de Puebla y Oaxaca. *Rev. Mex. Cienc. Geol.* **2**, 112–131 (1978).
16. Elías-Herrera, M. & Ortega-Gutiérrez, F. Caltepec fault zone: An Early Permian dextral transpressional boundary between the Proterozoic Oaxacan and Paleozoic Acatlán complexes, southern Mexico, and regional tectonic implications. *Tectonics* **21**, 1–18 (2002).
17. Solari, L. A. et al. 990 and 1100 Ma Grenvillian tectonothermal events in the northern Oaxacan complex, southern México: Roots of an orogen. *Tectonophysics* **365**, 257–282 (2003).
18. Tolson, G. La falla Chacalapa en el sur de Oaxaca. *Bol. Geol. Soc. Mex.* **57**, 111–122 (2005).
19. Talavera-Mendoza, O. et al. U–Pb geochronology of the Acatlán Complex and implications for the Paleozoic paleogeography and tectonic evolution of southern Mexico. *Earth. Planet. Sci. Lett.* **235**, 682–699 (2005).
20. Nance, R. D. et al. Acatlán Complex, southern Mexico: Record spanning the assembly and breakup of Pangea. *Geology* **34**, 857–860 (2006).
21. Keppie, J. D., Dostal, J., Murphy, J. B. & Nance, R. D. Synthesis and tectonic interpretation of the westernmost Paleozoic Variscan orogen in southern Mexico: From rifted Rheic margin to active Pacific margin. *Tectonophysics* **461**, 277–290 (2008).
22. Vega-Granillo, R. et al. Structural and tectonic evolution of the Acatlán Complex, southern Mexico: Its role in the collisional history of Laurentia and Gondwana. *Tectonics* **28**, 1–25 (2009).

23. Ortega-Gutiérrez, F. *et al.* Late Ordovician–Early Silurian continental collisional orogeny in southern Mexico and its bearing on Gondwana–Laurentia connections. *Geology* **27**, 719–722 (1999).
24. Ramos-Arias, M. A. & Keppie, J. D. U–Pb Neoproterozoic–Ordovician protolith age constraints for high- to medium-pressure rocks thrust over low-grade metamorphic rocks in the Ixcamilpa area, Acatlán Complex, southern Mexico. *Can. J. Earth. Sci.* **48**, 45–61 (2011).
25. Yáñez, P. *et al.* Isotopic studies of the Acatlán complex, southern Mexico: Implications for Paleozoic North American tectonics. *Geol. Soc. Am. Bull.* **103**, 817–828 (1991).
26. Elías-Herrera, M. *et al.* Conflicting stratigraphic and geochronologic data from the Acatlán Complex: “Ordovician” granites intrude sedimentary and metamorphic rocks of Devonian–Permian age. *Eos Trans. AGU 88 Jt. Assem. Suppl.* (Abstract T41A–12) (2001).
27. Ravna, E. J. & Terry, M. P. Geothermobarometry of UHP and HP eclogites and schists—an evaluation of equilibria among garnet–clinopyroxene–kyanite–phengite–coesite/quartz. *J. Metamorph. Geol.* **22**, 579–592 (2004).
28. Ravna, E. J. The garnet–clinopyroxene Fe²⁺–Mg geothermometer: An updated calibration. *J. Metamorph. Geol.* **18**, 211–219 (2000).
29. Nakamura, D. A new formulation of garnet–clinopyroxene geothermometer based on accumulation and statistical analysis of a large experimental data set. *J. Metamorph. Geol.* **27**, 495–508 (2009).
30. Sudholz, Z. J., Green, D. H., Yaxley, G. M. & Jaques, A. L. Mantle geothermometry: Experimental evaluation and recalibration of Fe–Mg geothermometers for garnet–clinopyroxene and garnet–orthopyroxene in peridotite, pyroxenite and eclogite systems. *Contrib. Mineral. Petrol.* **177**, 1–19 (2022).
31. Holt, A. F. & Condit, C. B. Slab temperature evolution over the lifetime of a subduction zone. *Geochem. Geophys. Geosyst.* **22**, 9476. <https://doi.org/10.1029/2020GC009476> (2021).
32. Guillot, S., Hattori, K., Agard, P., Schwartz, S. & Vidal, O. Exhumation processes in oceanic and continental subduction contexts: a review. In *Subduction Zone Geodynamics* (eds Lallemand, S. & Funicello, F.) 175–205 (Springer, 2009).
33. Powell, R. & Holland, T. J. B. On thermobarometry. *J. Metamorph. Geol.* **26**, 155–179 (2008).
34. Hacker, B. R. Pressures and temperatures of ultrahigh-pressure metamorphism: Implications for UHP tectonics and H₂O in subducting slabs. *Int. Geol. Rev.* **48**, 1053–1066 (2006).
35. Hernández-Urbe, D. & Palin, R. M. Catastrophic shear-removal of subcontinental lithospheric mantle beneath the Colorado Plateau by the subducted Farallon slab. *Sci. Rep.* **9**, 8153. <https://doi.org/10.1038/s41598-019-44628-y> (2019).
36. Hirajima, T. Effect of jadeite-content on the garnet–clinopyroxene geothermometer for an ultrahigh-pressure eclogite complex. *Proc. Jpn. Acad. B Phys.* **72**, 208–213 (1996).
37. Ravna, E. J. K. & Paquin, J. Thermobarometric methodologies applicable to eclogites and garnet ultrabasites. In *Ultrahigh Pressure Metamorphism* (eds Carswell, D. *et al.*) 229–259 (Mineralogical Society of Great Britain and Ireland, 2003).
38. Warr, L. N. IMA–CNMNC approved mineral symbols. *Mineral. Mag.* **85**, 291–320 (2021).
39. Waters, D. J. & Martin, H. N. Geobarometry of phengite-bearing eclogites. *Terra Abstracts* **5**, 410–411 (1993).
40. Cuthbert, S. J., Carswell, D. A., Krogh-Ravna, E. J. & Wain, A. Eclogites and eclogites in the Western Gneiss region, Norwegian Caledonides. *Lithos* **52**, 165–195 (2000).
41. Proyer, A., Dachs, E. & McCammon, C. Pitfalls in geothermobarometry of eclogites: Fe³⁺ and changes in the mineral chemistry of omphacite at ultrahigh pressures. *Contrib. Mineral. Petrol.* **147**, 305–318 (2004).
42. Rubatto, D. & Hermann, J. Exhumation as fast as subduction?. *Geology* **29**, 3–6 (2001).

Acknowledgements

Reviews by Tim Johnson and an anonymous reviewer greatly improved the manuscript and are gratefully acknowledged. Zheng-Xiang Li is thanked for editorial handling. M. M. Almazán-López, V. Colás, M. Elías-Herrera, F. Gutiérrez-Aguilar, C. Macias-Romo, F. Ortega-Gutiérrez, and M. Ramos-Arias are acknowledged for stimulating discussion about the Acatlán Complex. A. Victoria-Morales is thanked for introducing the author to the field area. F. Ortega-Gutiérrez is thanked for sharing the microprobe analyses of sample 152 and valuable comments in early versions of this work.

Author contributions

D.H.U. performed the calculations, interpreted the results, prepared, and reviewed the manuscript.

Competing interests

The author declares no competing interests.

Additional information

Supplementary Information The online version contains supplementary material available at <https://doi.org/10.1038/s41598-022-25992-8>.

Correspondence and requests for materials should be addressed to D.H.-U.

Reprints and permissions information is available at www.nature.com/reprints.

Publisher’s note Springer Nature remains neutral with regard to jurisdictional claims in published maps and institutional affiliations.



Open Access This article is licensed under a Creative Commons Attribution 4.0 International License, which permits use, sharing, adaptation, distribution and reproduction in any medium or format, as long as you give appropriate credit to the original author(s) and the source, provide a link to the Creative Commons licence, and indicate if changes were made. The images or other third party material in this article are included in the article’s Creative Commons licence, unless indicated otherwise in a credit line to the material. If material is not included in the article’s Creative Commons licence and your intended use is not permitted by statutory regulation or exceeds the permitted use, you will need to obtain permission directly from the copyright holder. To view a copy of this licence, visit <http://creativecommons.org/licenses/by/4.0/>.

© The Author(s) 2022